

Network Structure Identification from Corrupt Data Streams

Venkat Ram Subramanian, Andrew Lamperski, and Murti V. Salapaka

Abstract—Complex networked systems can be modeled as graphs with nodes representing the agents and links describing the dynamic coupling between them. Previous work on network identification has shown that the network structure of linear time-invariant (LTI) systems can be reconstructed from the joint power spectrum of the data streams. These results assumed that data is perfectly measured. However, real-world data is subject to many corruptions, such as inaccurate time-stamps, noise, and data loss. We show that identifying the structure of linear time-invariant systems using corrupt measurements results in the inference of erroneous links. We provide an exact characterization and prove that such erroneous links are restricted to the neighborhood of the perturbed node. We extend the analysis of LTI systems to the case of Markov random fields with corrupt measurements. We show that data corruption in Markov random fields results in spurious probabilistic relationships in precisely the locations where spurious links arise in LTI systems.

I. INTRODUCTION

Identification of network interaction structures is important for several domains such as climate science [1], epidemiology [2], neuroscience [3], metabolic pathways [4], quantitative finance [5] [6], the internet-of-things [7] [8] and video streaming [9]. In scenarios such as the power grid [10] and financial markets it is impractical, impossible or impermissible to externally influence the system. Here network structure identification must be achieved via passive means. The passive identification of a network of dynamically related agents is becoming more viable with sensors and measurements becoming inexpensive coupled with the ease and capability of communicating information.

Often, the measurements in such large systems are subjected to effects of noise [11], asynchronous sensor clocks [12] and packet drops [13]. When dealing with problems of identifying structural and functional connectivity of a large network, there is a pressing need to rigorously study such uncertainties and address detrimental effects of corrupt data-streams on network reconstruction. Such analysis can delineate the effects of corrupted nodes on the quality of the network reconstruction and suggest placement of high-fidelity sensors at critical nodes.

A. Related Work

Network identification for linear systems has been extensively studied. Below, we will give an overview of several research themes in linear system network identification. However, the majority of works assume that the measurements are perfect.

The authors are with the Department of Electrical and Computer Engineering, University of Minnesota, Minneapolis, MN 55455, USA. subra148@umn.edu, alampers@umn.edu, murtis@umn.edu

Work supported in part by NSF CMMI 1727096.

Identifiability conditions for determining the transfer functions are provided in [14]. It is shown that a network is identifiable if every node signal is excited by either an external input or a noise signal that is uncorrelated with the input/noise signals on the other nodes. The effects of data corruption are not studied in this work.

For partially observed states, authors in [15] provide necessary and sufficient conditions for *generic* identifiability of all or a subset of the transfer functions in the network. Similarly, the notion of *global* identifiability has been studied in [16]. However, in both the articles, the topology of the network is assumed to be known a priori. Moreover, data measurements are assumed to be perfect.

The problem of learning polytree structures has been studied in [17] and [18]. The authors provide guarantees of a consistent reconstruction. However, the class of network structures was restricted to trees and the data measurements are assumed to be ideal. In this article, we make no such assumptions on network structures and we study the problem when time-series data measurements are imperfect.

Authors in [19] leveraged multivariate Wiener filters to reconstruct the undirected topology of the generative network model. With assumptions of perfect measurements, and linear time invariant interactions, it is established that the multivariate Wiener filter can recover the *moral graph*. In other words, for each node, its parents, co-parents and children are detected.

For a network of interacting agents with nonlinear dynamics and strictly causal interactions, the authors in [20] proposed the use of directed information to determine the directed structure of the network. Here too, it is assumed that the data-streams are ideal with no distortions.

The authors in [21], [22] use dynamical structure functions (DSF) for network reconstruction [23] and consider measurement noise and non-linearities in the network dynamics. The proposed method first finds optimal DSF for all possible Boolean structures and then adopt a model selection procedure to determine the best estimate. The authors concluded that the presence of noise and non-linearities can even lead to spuriously inferring fully connected network structures. Also, the authors concluded that the performance of their algorithms degrades as noise, network size and non-linearities increase. However, a precise characterization of such spurious inferences in structure was not provided.

B. Our Contribution

In this article, our problem of interest is to determine the Boolean structure of a network, using passive means from corrupt data-streams and characterize the spurious links that can appear due to data-corruption.

In order to rigorously model data corruption, we present a general class of signal disturbance models based on random-

ized state-space systems. This class of disturbances subsumes many uncertainties that are prevalent in applications. We provide a detailed description on how the corruption model affects the second order statistics of the data-streams.

Next, we present the results for inferring the network topology for LTI systems from corrupt data-streams. Specifically, we identify a set of edges in the network in which spurious links could potentially appear. The results can be utilized to understand what part of the reconstruction can be trusted and to allocate sensor resources in order to minimize the effects of data corruption.

Finally, we extend our analysis and provide connections with more general graphical models. We prove that there can be spurious edges inferred during structure identification of undirected Markov random fields from corrupt data. The results characterizing the location of the spurious links are found to be identical to those obtained in LTI systems.

This paper is an extension of our earlier work [24] wherein preliminary results characterizing the spurious links were presented. However, a rigorous description on the perturbation models was not provided, and the work did not cover Markov random fields.

C. Paper Organization

We start by reviewing earlier work on LTI network identification using power spectra in Section II. In Section III, we describe our data corruption models. In Section IV, we characterize the spurious links due to data corruption for LTI systems. Section V discusses the effects of data-corruption in inferring the undirected structure of a Markov random field. Simulation results are provided in Section VI. Finally, a conclusion is provided in Section VII.

D. Notation

Y denotes a vector with y_i being i^{th} element of Y .

$z_i[\cdot]$ denotes a sequence and $z_{i,t}$ denotes $z_i[t]$.

$\|\cdot\|$ denotes standard Euclidian norm for vectors.

P_X represents the probability density function of a random variable X .

$X \perp\!\!\!\perp Y$ denotes that the random variables X and Y are independent.

$i \rightarrow j$ indicates an arc or edge from node i to node j in a directed graph.

$i - j$ denotes an undirected edge between nodes i, j in an undirected graph.

If $M(z)$ is a transfer function matrix, then $M(z)^* = M(z^{-1})^T$ is the conjugate transpose.

$\mathbb{E}[\cdot]$ denotes expectation operator.

$R_{XY}(k) := \mathbb{E}[X[n+k]Y[n]]$ is the cross-correlation function of jointly wide-sense stationary (WSS) processes X and Y . If $Y = X$ then $R_{XX}(k)$ is called the auto-correlation.

$\Phi_{XY}(z) := \mathcal{Z}(R_{XY}(k))$ represents the cross-power spectral density while $\Phi_{XX}(z) := \mathcal{Z}(R_{XX}(k))$ denotes the power spectral density (PSD) where $\mathcal{Z}(\cdot)$ is the Z-transform operator. b_i represents the i^{th} element of the canonical basis of \mathbb{R}^n .



Fig. 1: 1a Directed Graph and 1b its moral Graph.

II. BACKGROUND ON LTI NETWORK IDENTIFICATION

This section reviews earlier results on network identification from ideal data streams. See [19]. Required graph theoretic notions are described in Subsection II-A. The formal model of networked LTI systems is presented in Subsection II-B. Then, a result on network identification via power spectra is given in Subsection II-C. In later sections, we will analyze these results in the case that data has been corrupted.

A. Graph Theoretic Preliminaries

We will review some terminology from graph theory needed to describe the background results on LTI identification. For reference, see [25].

Definition 1 (Directed and Undirected Graphs). A directed graph G is a pair (V, A) where V is a set of vertices or nodes and A is a set of edges given by ordered pairs (i, j) where $i, j \in V$. If $(i, j) \in A$, then we say that there is an edge from i to j . (V, A) forms an undirected graph if V is a set of nodes or vertices and A is a set of the un-ordered pairs $\{i, j\}$.

We also denote an undirected edge as $i - j$.

Definition 2 (Children and Parents). Given a directed graph $G = (V, A)$ and a node $j \in V$, the children of j are defined as $\mathcal{C}(j) := \{i | j \rightarrow i \in A\}$ and the parents of j as $\mathcal{P}(j) := \{i | i \rightarrow j \in A\}$.

Definition 3 (Kins). Given a directed graph $G = (V, A)$ and a node $j \in V$, kins of j are defined as $\mathcal{K}_j := \{i | i \neq j \text{ and } i \in \mathcal{C}(j) \cup \mathcal{P}(j) \cup \mathcal{P}(\mathcal{C}(j))\}$. Kins are formed by parents, children and spouses. A spouse of a node is another node where both nodes have at-least one common child.

Definition 4 (Moral-Graph). Given a directed graph $G = (V, A)$, its moral-graph is the undirected graph $G^M = (V, A^M)$ where $A^M := \{\{i, j\} | j \in V, i \in \mathcal{K}_j\}$.

Fig. 1 provides an example of a directed graph and its moral graph.

B. Dynamic Influence Model for LTI systems

Here the generative model that is assumed to generate the measured data is described. Consider N agents that interact over a network. For each agent i , we associate an observable discrete time sequence $y_i[\cdot]$ and a hidden noise sequence $e_i[\cdot]$. The process $e_i[\cdot]$ is considered innate to agent i and thus e_i is independent of e_j if $i \neq j$. We assume e_i and y_i to be jointly wide-sense stationary stochastic processes. In particular, we

assume they are bounded in a mean-square sense: $\mathbb{E}[\|y_i[t]\|^2] < \infty$ and $\mathbb{E}[\|e_i[t]\|^2] < \infty$.

Let Y denote the set of all random process $\{y_1, \dots, y_N\}$ with a parent set $\mathcal{P}'(i)$ defined for $i = 1, \dots, N$. The parent set $\mathcal{P}'(i)$ associated with agent i does not include i . The process y_i depends dynamically on the processes of its parents, y_j with $j \in \mathcal{P}'(i)$ through an LTI filter whose impulse response is given by \mathcal{G}_{ij} . Therefore, dynamics of node i takes the form:

$$y_i[t] = \sum_{j \in \mathcal{P}'(i)} (\mathcal{G}_{ij} * y_j)[t] + e_i[t] \quad \text{for } i = 1, \dots, N. \quad (1)$$

where $*$ denotes convolution operation. Performing a Z -transform on both sides gives

$$y_i(z) = \sum_{j \in \mathcal{P}'(i)} \mathcal{G}_{ij}(z)y_j(z) + e_i(z) \quad \text{for } i = 1, \dots, N. \quad (2)$$

For compact notation, we will often drop the z arguments. Let $y = (y_1, y_2, \dots, y_N)^T$ and $e = (e_1, e_2, \dots, e_N)^T$. Then (2) is equivalent to

$$y = \mathcal{G}(z)y + e. \quad (3)$$

The diagonal entries $\mathcal{G}_{ii}(z)$ are considered to be zero. We refer to (3) as the Dynamic Influence Model (DIM). Here, \mathcal{G} is termed as the DIM generative connectivity matrix. The DIM will be denoted by (\mathcal{G}, e) .

Remark 1. The process noise in (1) can be correlated across time. In that case, e_i is assumed to be represented as the convolution of white noise with a stable LTI filter.

Remark 2. The diagonal entries, $\mathcal{G}_{ii}(z)$ are considered to be zero only for simplification purposes to remove self-dependence in the dynamics. As will be seen later in subsection II-C, this enables us to consider Wiener filter projection of signal y_i on all signals except y_i . Moreover, we can model the self-dependence and include it in the DIM through the process noise sequence by convolving a zero mean white noise with $\mathcal{G}_{ii}(z)$.

We illustrate the notation by an example. Consider a network of five agents whose node dynamics are given by,

$$\begin{aligned} y_1 &= e_1 \\ y_2 &= \mathcal{G}_{21}(z)y_1 + e_2 \\ y_3 &= \mathcal{G}_{31}(z)y_1 + e_3 \\ y_4 &= \mathcal{G}_{42}(z)y_2 + \mathcal{G}_{43}(z)y_3 + e_4 \\ y_5 &= \mathcal{G}_{54}(z)y_4 + e_5 \end{aligned} \quad (4)$$

$$\text{with } \mathcal{G} = \begin{bmatrix} 0 & 0 & 0 & 0 & 0 \\ \mathcal{G}_{21} & 0 & 0 & 0 & 0 \\ \mathcal{G}_{31} & 0 & 0 & 0 & 0 \\ 0 & \mathcal{G}_{42} & \mathcal{G}_{43} & 0 & 0 \\ 0 & 0 & 0 & \mathcal{G}_{54} & 0 \end{bmatrix}.$$

Definition 5 (Generative Graph). The structural description of (3) induces a generative graph $G = (V, A)$ formed by identifying each vertex v_i in V with random process y_i and

the set of directed links, A , obtained by introducing a directed link from every element in the parent set $\mathcal{P}'(i)$ of agent i to i .

Note that we do not show $i \rightarrow i$ in the generative graph and neither do we show the processes e_i . The generative graph associated with the examples described in (4) is given by Fig. 1 (a).

C. Identification from Ideal Measurements

The following results are obtained from [19] where the authors have leveraged Wiener filters for determining generative graphs of a DIM.

Theorem 1. Consider a DIM (\mathcal{G}, e) consisting of N nodes with generative graph G . Let the output of the DIM be given by $y = (y_1, \dots, y_N)^T$. Suppose that S_j is the span of all random variables $y_k[t]$, $t = \dots, -2, -1, 0, 1, 2, \dots$ excluding y_j . Define the estimate \hat{y}_j of the time-series y_j via the optimization problem of

$$\min_{\hat{y}_j \in S_j} \mathbb{E} \left[(y_j - \hat{y}_j)^T (y_j - \hat{y}_j) \right].$$

Then a unique optimal solution to the above exists and is given by

$$\hat{y}_j = \sum_{i \neq j} \mathbf{W}_{ji}(z)y_i \quad (5)$$

where $\mathbf{W}_{ji}(z) \neq 0$ implies $y_i \in \mathcal{K}_{y_j}$ (equivalently $y_j \in \mathcal{K}_{y_i}$); that is i is a kin of j .

The solution in (5) is the Wiener Filter solution which is given by $\Phi_{y_j y_j}^{-1} \Phi_{y_j y_j}^{-1}$ where y_j denotes the vector of all processes excluding y_j and Φ denotes the power spectral density. Thus, Theorem 1 implies that we can reconstruct the moral graph of a DIM by analyzing the joint power spectral density of the measurements. The following corollary gives a useful characterization of the inferred kin relationships in terms of the sparsity pattern of Φ_{yy}^{-1} .

Corollary 1. Under the assumptions of Theorem 1, let Φ_{yy} be the power spectral density matrix of the vector process y . Then the (j, i) entry of Φ_{yy}^{-1} is non zero implies that i is a kin of j .

Remark 3. $\Phi_{yy}^{-1}(i, j)$ is described by (i, j) entry of $(I - \mathcal{G}(z))^* \Phi_e^{-1} (I - \mathcal{G}(z))$. Specifically, $\Phi_{yy}^{-1}(i, j) = -\mathcal{G}_{ij} \phi_{e_i}^{-1} - \mathcal{G}_{ji}^* \phi_{e_j}^{-1} + \sum_k \mathcal{G}_{ki}^* \mathcal{G}_{kj} \phi_{e_k}^{-1}$ where $k \in \mathcal{C}(i) \cap \mathcal{C}(j)$. For i and j being kins but $\Phi_{yy}^{-1}(i, j)$ to be zero, the transfer functions in \mathcal{G} must belong to a set of measure zero on space of system parameters. For example, system dynamics with transfer functions being zero or a static system with all noise sequences being identical. Therefore, except for these restrictive cases, the results in Theorem 1 and Corollary 1 are both necessary and sufficient. See [19] for more details.

III. UNCERTAINTY DESCRIPTION

Subsection II-C describes a methodology from [19] for guaranteed kinship reconstruction based on Wiener filtering. However, the results assume that the signals, y_i , are measured perfectly. This paper aims to explain what would happen if

we attempted to apply the reconstruction method to data that has been corrupted. We will see that extra links appear in the reconstruction, and characterize the pattern of spurious links. While the analysis of the next two sections focuses on LTI identification, the results on Markov random fields in Section V indicate that the emergence and pattern of spurious links are general properties of network reconstruction from corrupted data.

Subsection III-A presents the general class of data corruption models studied for LTI systems. The modeling framework is sufficiently general to capture a variety of practically relevant perturbations, such as delays and packet loss. However, we will see that all of the corruption models have similar effects on the observed power spectra. Specific examples of perturbation models are described in Subsection III-B.

A. Random State Space Models

This subsection presents the general class of perturbation models. Consider i^{th} node in a network and let its associated unperturbed time-series be y_i . The corrupt data-stream u_i associated with i is considered to follow the stochastic linear system described below:

$$x_i[t+1] = A_i[t]x_i[t] + B_i[t]y_i[t] + w_i[t] \quad (6a)$$

$$u_i[t] = C_i[t]x_i[t] + D_i[t]y_i[t] + v_i[t], \quad (6b)$$

where x_i denotes hidden states in the stochastic linear system that describes the corruption. Here, the matrices, $M_i[t] = \begin{bmatrix} A_i[t] & B_i[t] \\ C_i[t] & D_i[t] \end{bmatrix}$ are independent, identically distributed (IID) and independent of $y_i[t]$. The terms $w_i[t]$ and $v_i[t]$ are zero-mean IID noise terms which are independent of $M_i[\cdot]$ and $y_i[\cdot]$ and have covariance:

$$\mathbb{E} \begin{bmatrix} w_i[t] \\ v_i[t] \end{bmatrix} \begin{bmatrix} w_i[t] \\ v_i[t] \end{bmatrix}^\top = \begin{bmatrix} W & S \\ S^\top & V \end{bmatrix}. \quad (7)$$

For distinct perturbed nodes, $i \neq j$, we assume that $M_i[\cdot]$, $w_i[\cdot]$, and $v_i[\cdot]$ are independent of $M_j[\cdot]$, $w_j[\cdot]$, and $v_j[\cdot]$.

Denote the means of the state space matrices by $\bar{A}_i = \mathbb{E}[A_i[t]]$, $\bar{B}_i = \mathbb{E}[B_i[t]]$, $\bar{C}_i = \mathbb{E}[C_i[t]]$, and $\bar{D}_i = \mathbb{E}[D_i[t]]$.

Let h_i be the impulse response of the system defined by $\bar{A}_i, \bar{B}_i, \bar{C}_i, \bar{D}_i$:

$$h_i(k) = \left[\begin{array}{c|c} \bar{A}_i & \bar{B}_i \\ \hline \bar{C}_i & \bar{D}_i \end{array} \right] (k) \quad (8)$$

Note that $\bar{u}_i[t] = \mathbb{E}[u_i[t]|y_i] = (h_i \star y_i)[t]$.

Theorem 2. Assume that $M_i[t]$ has bounded second moments and for all positive definite matrices Q , the following generalized Lyapunov equation has a unique positive definite solution, P :

$$P = \mathbb{E}[A_i[t]PA_i[t]^\top] + Q. \quad (9)$$

Define $\Delta u_i[t] := u_i[t] - \bar{u}_i[t]$. Then, the signals u_i will be wide sense-stationary with cross-spectra and power spectra of the form:

$$\Phi_{u_i u_i}(z) = H_i(z)\Phi_{y_i y_i}(z)H_i(z^{-1}) + \theta_i(z) \quad (10a)$$

$$\Phi_{u_i y_i}(z) = H_i(z)\Phi_{y_i y_i}(z) \quad (10b)$$

where, $H_i(z) = \mathcal{Z}(h_i)$ and $\theta_i(z) = \mathcal{Z}(R_{\Delta u_i \Delta u_i}[k])$.

The proof is given in Appendix A.

B. Data Corruption Examples

We will highlight a few corruptions that are practically relevant to exemplify the above model description. More complex perturbations can be obtained by composing these models.

1) *Random Delays*: Randomized delays can be modeled by

$$u_i[t] = y_i[t - d[t]] \quad (11)$$

where $d[t]$ is a random variable. For example, if $d[t] \in \{1, 2, 3\}$, then randomized delay model can be represented in state-space form with no additive noise terms and state space matrices given by:

$$\begin{bmatrix} A_i[t] & B_i[t] \\ C_i[t] & D_i[t] \end{bmatrix} = \begin{bmatrix} \begin{bmatrix} 0 & 0 & 0 \\ 1 & 0 & 0 \\ 0 & 1 & 0 \end{bmatrix} & \begin{bmatrix} 1 \\ 0 \\ 0 \end{bmatrix} \\ -b_{d[t]}^\top & 0 \end{bmatrix},$$

where b_1, b_2 , and b_3 are the standard basis vectors of \mathbb{R}^3 .

Say that $d[t] = j$ with probability p_j , for $j = 1, 2, 3$. Then

$$H_i(z) = p_1 z^{-1} + p_2 z^{-2} + p_3 z^{-3}. \quad (12)$$

Let $p = [p_1 \ p_2 \ p_3]$. The formal description to compute the expression for $\theta_i(z)$ is discussed in Lemma 3 contained in the Appendix section. Using Lemma 3 we have that $R_{\Delta u_i \Delta u_i}[t] = 0$ for $t \neq 0$ and $R_{\Delta u_i \Delta u_i}[0]$ is given by

$$R_{y_i y_i}[0] - p^\top \begin{bmatrix} R_{y_i y_i}[0] & R_{y_i y_i}[1] & R_{y_i y_i}[2] \\ R_{y_i y_i}[-1] & R_{y_i y_i}[0] & R_{y_i y_i}[1] \\ R_{y_i y_i}[-2] & R_{y_i y_i}[-1] & R_{y_i y_i}[0] \end{bmatrix} p. \quad (13)$$

2) *Measurement Noise*: White measurement noise can be represented in the form of (6) by setting $C_i[t] = 0$, $D_i[t] = 1$:

$$u_i[t] = y_i[t] + v_i[t]. \quad (14)$$

Colored measurement noise with rational spectrum arises when $B_i[t] = 0$, $D_i[t] = 1$, and the matrices $A_i[t]$ and $C_i[t]$ are constant. More generally, the result of causally filtering the signal and then adding noise can be modeled by taking all of the matrices in (6) to be constant.

For the corruption model described in (14), the perturbation transfer functions are given by:

$$H_i(z) = 1 \\ \theta_i(z) = \Phi_{v_i v_i}(z).$$

3) *Adversarial Disinformation*: This is an example of data-corruption that is pertinent to cyber-security. Here, the true data stream y_i is completely concealed and a new false data stream v_i is introduced. This is an extreme case of (6) in which $C_i[t]$ and $D_i[t]$ are zero:

$$u_i[t] = v_i[t] \quad (15)$$

4) *Packet Drops*: Here the data stream suffers from randomly dropping measurement packets. The corrupted data stream u_i is obtained from y_i as follows:

$$u_i[t] = \begin{cases} y_i[t], & \text{with probability } p_i \\ u_i[t-1], & \text{with probability } (1-p_i) \end{cases} \quad (16)$$

Packet drops can be modeled in the form of (6) with no noise and matrices given by:

$$\begin{bmatrix} A_i[t] & B_i[t] \\ C_i[t] & D_i[t] \end{bmatrix} = \begin{cases} \begin{bmatrix} 0 & 1 \\ 0 & 1 \end{bmatrix} & \text{with probability } p_i \\ \begin{bmatrix} 1 & 0 \\ 1 & 0 \end{bmatrix} & \text{with probability } 1-p_i. \end{cases} \quad (17)$$

The generalized Lyapunov equation becomes:

$$P = p_i P \cdot 0 + (1-p_i) P \cdot 1 + Q \quad (18)$$

which has the solution $P = Q/p_i$. Thus, the conditions for Theorem 2 hold, and so u_i is wide-sense stationary. In this case

$$\begin{bmatrix} \bar{A}_i & \bar{B}_i \\ \bar{C}_i & \bar{D}_i \end{bmatrix} = \begin{bmatrix} 1-p_i & p_i \\ 1-p_i & p_i \end{bmatrix} \quad (19)$$

so that $H_i(z) = \frac{p_i(1-p_i)}{z-(1-p_i)} + p_i = \frac{p_i}{1-z^{-1}(1-p_i)}$.

The formal description to compute the expression for $\theta_i(z)$ is discussed in Lemma 3 contained in the Appendix section. The application of methods described in the Appendix to derive an expression for $\theta_i(z)$ is cumbersome. However, $\theta_i(z)$ can be calculated directly. Indeed, direct calculation shows that

$$(h_i \star R_{yy} \star h_i^*)[t] = \sum_{j=-\infty}^{|t|} \sum_{k=j}^{\infty} p_i^2 (1-p_i)^{|t|+k-2j} R_{yy}[k] \quad (20)$$

while inductive application of (16) shows that

$$R_{uu}[t] = (1-p_i)^{|t|} R_{yy}[0] + \sum_{j=1}^{|t|} \sum_{k=j}^{\infty} p_i^2 (1-p_i)^{|t|+k-2j} R_{yy}[k]. \quad (21)$$

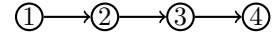
Here, the sum is interpreted as 0 when $|t| = 0$.

Subtracting (20) from (21) and taking Z -transforms gives

$$\theta_i(z) = \frac{(1-p_i)^2}{(1-z^{-1}(1-p_i))(1-z(1-p_i))} \left(R_{yy}[0] + \sum_{j=-\infty}^{\infty} \sum_{k=j}^{\infty} p_i^2 (1-p_i)^{k-2j} R_{yy}[k] \right). \quad (22)$$

IV. SPURIOUS LINKS FOR PERTURBED LTI SYSTEMS

The results reviewed from [19] imply that kin relationships could be inferred from the power spectra of ideal measurements. However, the result of Theorem 2 implies that common types of data corruption cause perturbations to the power spectrum of the observations. In this section, we will show how use of the method from [19] on corrupted data streams leads to the inference of spurious links. In Subsection IV-A we show how spurious links arise in a simple example. Then in



(a) Perfect Measurements



(b) Unreliable Measurements

Fig. 2: When node 2 has corrupt measurements an external observer might wrongly infer that the third node is directly influenced by node 1.

Subsection IV-B, we characterize the pattern of spurious links that could arise due to data corruption. While these results in this section are specific to the power spectrum inference method from [19], the work in Section V shows that the pattern of spurious links arises more generally in network identification problems.

A. Example: Spurious Links due to Data Corruption

Before presenting the general results, an example will be described. Consider the generative graph of a directed chain in Figure 2a. Suppose the measured data-streams are denoted by u_i for node i where $u_i = y_i$ for $i = 1, 3, 4$ (thus no data uncertainty at nodes 1, 3 and 4) and u_2 is related to y_2 via the randomized delay model described in (11). In this case, the processes u_i are jointly WSS and the PSD of the vector process $u = (u_1, \dots, u_4)^T$ is related to the PSD of the vector process y via:

$$\Phi_{uu}(z) = \underbrace{\begin{bmatrix} 1 & 0 & 0 & 0 \\ 0 & h_2(z) & 0 & 0 \\ 0 & 0 & 1 & 0 \\ 0 & 0 & 0 & 1 \end{bmatrix}}_{H(z)} \Phi_{yy}(z) \underbrace{\begin{bmatrix} 1 & 0 & 0 & 0 \\ 0 & h_2(z^{-1}) & 0 & 0 \\ 0 & 0 & 1 & 0 \\ 0 & 0 & 0 & 1 \end{bmatrix}}_{H^*(z)} + \underbrace{\begin{bmatrix} 0 & 0 & 0 & 0 \\ 0 & \theta_2(z) & 0 & 0 \\ 0 & 0 & 0 & 0 \\ 0 & 0 & 0 & 0 \end{bmatrix}}_{\mathcal{D}},$$

where h_2 and θ_2 were described in Subsection III.

Note that $\mathcal{D} = b_2 \theta_2 b_2^T$, where $b_2 = (0 \ 1 \ 0 \ 0)^T$. Set $\Psi(z) = H(z) \Phi_{yy}(z) H^*(z)$. It follows from the Woodbury matrix identity [26] that

$$\Phi_{uu}^{-1}(z) = \Psi^{-1}(z) - \Psi^{-1}(z) b_2 b_2^T \Psi^{-1}(z) \Delta^{-1}, \quad (23)$$

where $\Delta = \theta_2^{-1} + b_2^T \Psi^{-1}(z) b_2$ is a scalar.

Corollary 1 implies that the sparsity pattern of $\Phi_{yy}^{-1}(z)$ is given by:

$$\Phi_{yy}^{-1}(z) = \begin{bmatrix} * & * & 0 & 0 \\ * & * & * & 0 \\ 0 & * & * & * \\ 0 & 0 & * & * \end{bmatrix} \quad (24)$$

where $*$ indicates a potential non-zero entry.

Since $H(z)$ is diagonal, it follows that $\Psi^{-1}(z)$ and $\Phi_{yy}^{-1}(z)$ have the same sparsity pattern. Thus, the sparsity pattern of $\Psi^{-1}(z)b_2$ and $\Psi^{-1}(z)b_2b_2^T\Psi^{-1}(z)$ are given by:

$$\Psi^{-1}(z)b_2 = \begin{bmatrix} * \\ * \\ * \\ 0 \end{bmatrix}, \quad \Psi^{-1}(z)b_2b_2^T\Psi^{-1}(z) = \begin{bmatrix} * & * & * & 0 \\ * & * & * & 0 \\ * & * & * & 0 \\ 0 & 0 & 0 & 0 \end{bmatrix} \quad (25)$$

Combining (23)-(25), it follows that the $\Phi_{uu}^{-1}(z)$ has sparsity pattern given by:

$$\Phi_{uu}^{-1}(z) = \begin{bmatrix} * & * & * & 0 \\ * & * & * & 0 \\ * & * & * & * \\ 0 & 0 & * & * \end{bmatrix}.$$

The extra filled spot in the inverse power spectral density corresponds to a spurious link. See Fig. 2.

B. Determining Generative Topology from Corrupted Data Streams

In this subsection, we will generalize the insights from the preceding subsection to arbitrary DIMs. The following definitions are needed for the development to follow.

Definition 6 (Path and Intermediate nodes). *Nodes $v_1, v_2, \dots, v_k \in V$ forms a path from v_1 to v_k in an undirected graph $G = (V, A)$ if for every $i = 1, 2, \dots, k-1$ we have $v_i - v_{i+1}$. The nodes v_2, v_3, \dots, v_{k-1} are called the intermediate nodes in the path.*

Definition 7 (Neighbors \mathcal{N}). *Let $G = (V, A)$ be an undirected graph. The neighbor set of node i is given by $\mathcal{N} = \{j : i-j \in A\} \cup \{i\}$.*

Definition 8 (Erroneous Links). *Let $G = (V, A)$ be an undirected graph. An edge or arc $i-j$ is called an erroneous link when it does not belong to A where $i, j \in V$.*

Definition 9 (Perturbed Graph). *Let $G = (V, A)$ be an undirected graph. Suppose $Z \subset V$ is the set of perturbed nodes. Then the perturbed graph of G with respect to set Z is the graph $G_Z = (V, A_Z)$ such that $i-j \in A_Z$ if either $i-j \in A$ or there is a path from i to j in G such that all intermediate nodes are in Z .*

Note that if $Z \subset \hat{Z}$, then $A_Z \subset A_{\hat{Z}}$.

The following theorem is the main result for LTI identification.

Theorem 3. *Consider a DIM (\mathcal{G}, e) consisting of N nodes with the moral graph $G^M = (V, A^M)$. Let $Z = \{v_1, v_2, \dots, v_n\}$ be the set of n perturbed nodes where each perturbation satisfies (10). Then $(\Phi_{uu}^{-1}(z))_{pq} \neq 0$ implies that p and q are neighbors in the perturbed graph G_Z^M .*

Proof. First, we will describe the structure of $\Phi_{uu}(z)$. For compact notation, we will often drop the z arguments.

For $p = 1, \dots, N$, if p is not a perturbed node, set $H_p(z) = 1$ and $\theta_p(z) = 0$. With this notation, (10) implies that the entries of Φ_{uu} are given by:

$$(\Phi_{uu})_{pq} = \begin{cases} H_p(\Phi_{yy})_{pq}H_q^* & \text{if } p \neq q \\ H_p(\Phi_{yy})_{pp}H_p^* + \theta_p & \text{if } p = q \end{cases}$$

When $p \neq q$, there is no θ term because the perturbations were assumed to be independent.

In matrix notation, we have that:

$$\Phi_{uu} = H\Phi_{yy}H^* + \sum_{k=1}^n \mathcal{D}_{v_k}$$

where H is the diagonal matrix with entries H_p on the diagonal and $\mathcal{D}_{v_k}(z) = b_{v_k}\theta_{v_k}(z)b_{v_k}^T$ where b_{v_k} is the canonical unit vector with 1 at entry v_k .

Set $\Psi_0 = H\Phi_{yy}H^*$. For $k = 0, \dots, n-1$, we can inductively define the matrices:

$$\Psi_{k+1} = \Psi_k + b_{v_{k+1}}\theta_{v_{k+1}}b_{v_{k+1}}^T \quad (26)$$

For $k = 1, \dots, n$ let $Z_k = \{v_1, \dots, v_k\}$ and let $G_{Z_k}^M$ be the perturbed graph constructed by adding edges $i-j$ to the original moral graph if there is a path from i to j whose intermediate nodes are all in Z_k .

We will inductively prove the following claim: For $k = 1, \dots, n$, if $(\Psi_k^{-1})_{pq} \neq 0$, then p and q are neighbors in $G_{Z_k}^M$. Proving this claim is sufficient to prove the theorem, since $\Psi_n = \Phi_{uu}$ and $Z_n = Z$.

First we focus on the $k = 1$ case. Using the Woodbury Matrix identity we have, $\Psi_1^{-1} = \Psi_0^{-1} - \Gamma_1$, where $\Gamma_1 := (\Psi_0^{-1}b_{v_1}b_{v_1}^T\Psi_0^{-1})\Delta_{v_1}^{-1}$ and $\Delta_{v_1} = \theta_{v_1}^{-1} + b_{v_1}^T\Psi_0^{-1}(z)b_{v_1}$ is a scalar. Therefore, $(\Psi_1^{-1})_{pq} = (\Psi_0^{-1})_{pq} - (\Gamma_1)_{pq}$.

If $(\Psi_1^{-1})_{pq} \neq 0$ then at least one of the conditions (i) $(\Psi_0^{-1})_{pq} \neq 0$ or (ii) $(\Gamma_1)_{pq} \neq 0$ must hold.

Suppose that $(\Psi_0^{-1})_{pq} \neq 0$. Then $(H^{-*}(z)\Phi_{yy}^{-1}H^{-1}(z))_{pq} \neq 0$. As H is diagonal it follows that $(\Phi_{yy}^{-1})_{pq} \neq 0$. From Corollary 1, it follows that p and q are neighbors in G^M . Thus p and q are neighbors in $G_{B_1}^M$.

Suppose that $(\Gamma_1)_{pq} \neq 0$. Then it follows that $(\Psi_0^{-1}b_{v_1}b_{v_1}^T\Psi_0^{-1})_{pq}\Delta_{v_1}^{-1} \neq 0$. Thus $(\Psi_0^{-1}b_{v_1})_p \neq 0$ and $(b_{v_1}^T\Psi_0^{-1})_q \neq 0$. Noting that $\Psi_0 = H\Phi_{yy}H^*$, it follows that $(\Phi_{yy}^{-1})_{pv_1} \neq 0$ and $(\Phi_{yy}^{-1})_{v_1q} \neq 0$. From Corollary 1 it follows that v_1-p and v_1-q are edges in the moral graph G^M . Thus, there is a path from p to q whose only intermediate node is $v_1 \in Z_1$. Thus, p, q are neighbors in $G_{Z_1}^M$ and the claim is verified for $k = 1$.

Now assume that the claim holds for some $k > 1$. Combining the Woodbury matrix identity with (26) implies that

$$\Psi_{k+1}^{-1} = \Psi_k^{-1} - \Gamma_{k+1}$$

where $\Gamma_{k+1} = \Psi_k^{-1}b_{v_{k+1}}b_{v_{k+1}}^T\Psi_k^{-1}\Delta_{v_{k+1}}^{-1}$ and $\Delta_{v_{k+1}} = \theta_{v_{k+1}}^{-1} + b_{v_{k+1}}^T\Psi_k^{-1}(z)b_{v_{k+1}}$ is a scalar.

As before, if $(\Psi_{k+1}^{-1})_{pq} \neq 0$, then either $(\Psi_k^{-1})_{pq} \neq 0$ or $(\Gamma_{k+1})_{pq} \neq 0$.

If $(\Psi_k^{-1})_{pq} \neq 0$, then the induction hypothesis implies that p and q are neighbors in $G_{Z_k}^M$. Since $Z_k \subset Z_{k+1}$, it follows that p and q are neighbors in $G_{Z_{k+1}}^M$.

If $(\Gamma_{k+1})_{pq} \neq 0$, then as in the $k = 1$ case, we must have that $(\Psi_k^{-1})_{pv_{k+1}} \neq 0$ and $(\Psi_k^{-1})_{v_{k+1}q} \neq 0$. This implies that $p - v_{k+1} \in A_{Z_k}^M$ and $v_{k+1} - q \in A_{Z_k}^M$. Thus, either p and v_{k+1} are kins in the original moral graph, or there is a path from p to v_{k+1} whose intermediate nodes are in Z_k . Similarly, for q and v_{k+1} . It follows that there is a path from p to q whose nodes are in Z_{k+1} , and thus p and q are neighbors in $G_{Z_{k+1}}^M$. The claim, and thus the theorem, are now proved. \square

Remark 4. Similar to Remark 3, cases where i and j are kins in the original moral graph, G^M , but $\Phi_{uu}^{-1}(i, j)$ is zero are pathological. $\Phi_{uu}^{-1}(i, j)$ is expressed by terms in $\Phi_{yy}^{-1}, H_l(z)$ and $\theta_l(z)$ where l is a perturbed node. As remarked earlier, the entries in $\mathcal{G}(z)$ and the corruption model described in (6) must belong to a set of measure zero on space of system parameters such that $\Phi_{uu}^{-1}(i, j)$ is zero. Therefore, except for these restrictive cases, the result in Theorem 3 implies that we can identify the perturbed kin graph.

V. SPURIOUS CORRELATIONS OF PERTURBED MARKOV RANDOM FIELDS

So far, we have shown how perturbing time-series data can give rise to spurious inferences. The analysis was restricted to network identification via Wiener filtering. In this section, we will show that spurious links arising from data corruption is a more general phenomenon. Specifically, we will show that the exact same patterns of spurious links from Theorem 3 will arise in a general class of probabilistic graphical models known as Markov random fields.

Markov random fields can model a variety of distributions, including continuous and discrete variables. However, our presentation here is restricted to finite-dimensional random variables with well defined probability mass or density functions. Thus, while the class is broad, it does not subsume the analysis from Section IV, which deals with infinite-dimensional time-series data. However, as we will see Markov random fields can model time-series analysis problems with finite amounts of data.

A. Background on Markov Random Fields

Our presentation of Markov random fields will be closely related to graph cliques:

Definition 10 (Clique). Given an undirected graph $G = (V, A)$, a clique is a complete sub-graph formed by a set of vertices $b \subset V$ such that for all distinct $i, j \in b$ there exists $i - j \in A$.

As an example of a Markov random field, consider a finite-dimensional version of the model from (4):

$$\begin{aligned} y_1 &= e_1 \\ y_2 &= M_{21}y_1 + e_2 \\ y_3 &= M_{31}y_1 + e_3 \\ y_4 &= M_{42}y_2 + M_{43}y_3 + e_4 \\ y_5 &= M_{54}y_4 + e_5 \end{aligned} \quad (27)$$

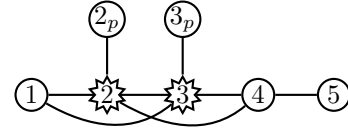


Fig. 3: Markov random field G^J with perturbed nodes.

with

$$M = \begin{bmatrix} 0 & 0 & 0 & 0 & 0 \\ M_{21} & 0 & 0 & 0 & 0 \\ M_{31} & 0 & 0 & 0 & 0 \\ 0 & M_{42} & M_{43} & 0 & 0 \\ 0 & 0 & 0 & M_{54} & 0 \end{bmatrix}.$$

Here, we take e_i to be independent Gaussian vectors with mean 0 and covariance E_i . When only a finite amount of time series data has been collected for the system in (4), the relationship between the data points can be modeled as in (27).

Now we will see how the structure of the probabilistic relationships between the variables, y_i are encoded in the corresponding moral graph from Fig. 1b. If $y = [y_1 \ \cdots \ y_5]^\top$ and $e = [e_1 \ \cdots \ e_5]^\top$, then $y = (I - M)^{-1}e$. Use the notation $\|x\|_{E_i}^2 = x^\top E_i^{-1}x$. Then direct calculation shows that the density of y factorizes as

$$\begin{aligned} p(y) &= c \cdot \exp \left(-\frac{1}{2} \|y_1\|_{E_1}^2 - \frac{1}{2} \|y_2 - M_{21}y_1\|_{E_2}^2 \right. \\ &\quad \left. - \frac{1}{2} \|y_3 - M_{31}y_1\|_{E_3}^2 \right) \cdot \\ &\quad \exp \left(-\frac{1}{2} \|y_4 - M_{42}y_2 - M_{43}y_3\|_{E_4}^2 \right) \cdot \\ &\quad \cdot \exp \left(-\frac{1}{2} \|y_5 - M_{54}y_4\|_{E_5}^2 \right). \end{aligned} \quad (28)$$

Note that the exponential factors contain variables $\{y_1, y_2, y_3\}$, $\{y_2, y_3, y_4\}$, and $\{y_4, y_5\}$. These variable groupings correspond precisely to the maximal cliques in the moral graph from Fig. 1b.

As we will discuss below, having a distribution that factorizes with respect to a graph is a sufficient condition for being a Markov random field. See also [27]. A generalization of the construction of (27) shows that finite collections of time-series data can always be viewed as Markov random fields.

To formally define Markov random fields, we need some extra notation and terminology. Let Y be a collection of variables, $Y = \{y_1, \dots, y_{|V|}\}$ corresponding to nodes of a graph, $G = (V, A)$. If $S \subset V$, then we use the notation $Y_S = \{y_i | i \in S\}$.

Definition 11 (Separation). Suppose $G = (V, A)$ is an undirected graph. Suppose, a, b, c are disjoint subsets of V . Then, a and b are separated given c if all paths from a to b must pass through c .

When a and b are separated given c , we write $\text{sep}(a, b | c)$.

Definition 12 (Markov random fields). Let Y be a collection of random variables associated with the nodes of an undirected graph, $G = (V, A)$. The variables Y are called a Markov

random field with respect to G if Y_a and Y_b are conditionally independent given Y_c whenever $\text{sep}(a, b | c)$ holds.

A useful sufficient condition for Y to be a Markov random field with respect to G is for the distribution to factorize into terms corresponding to cliques in the graph. This condition was used in the example above. See [27] for more details.

Definition 13 (Clique Factorization). *Suppose that Q is a collection of subsets of V such that each $q \in Q$ forms clique in G . Let $P(Y)$ denote the joint probability distribution of the random variables Y . Then, we say Y factorizes according to G , if for every $q \in Q$, there exists non-negative functions Ψ_q that are functions of random variables in q such that,*

$$P(Y) = \prod_{q \in Q} \Psi_q(Y_q) \quad (29)$$

B. Inferring Erroneous Links

Now we will describe the effects of data-corruption on inferring the undirected graph structure from measured data. In our work on time-series models, we assumed that individual data streams were perturbed independently. Here we will define a natural analog of independent perturbations for Markov random fields. However, the perturbation models could be non-linear.

Let Y be a Markov random field that factorizes with respect to a graph $G = (V, A)$. Let $Z \subset V$ be the set of perturbed nodes. For each perturbed node, $i \in Z$, we draw a new node i_p , draw an edge $i-i_p$, and denote the corresponding perturbed variable by u_i . The probabilistic relationships between the original variable, y_i , and the perturbed variable, u_i , is given by $\Psi_{ii_p}(y_i, u_i) \geq 0$. Let $Z_p = \{i_p : i \in Z\}$ and let U_Z denote the set of perturbed variables. Then the joint distribution between Y and U_Z can be described as:

$$P(Y, U_Z) = \prod_{q \in Q} \Psi_q(Y_q) \cdot \prod_{i \in Z} \Psi_{ii_p}(y_i, u_i). \quad (30)$$

Since the node pairs, $\{i, i_p\}$ are cliques, the construction above shows that the joint variables (Y, U_Z) form a Markov random field with respect to $G^J = (V \cup Z_p, A \cup \{i - i_p : \forall i \in Z\})$. See figure 3.

Due to data corruption, only the variables $Y_{\bar{Z}}$ and U_Z are observed, where $\bar{Z} = V \setminus Z$. The next lemma shows that $(Y_{\bar{Z}}, U_Z)$ is also a Markov random field, with graph described by the perturbed graph.

Lemma 1. *Let Y be a Markov random field with respect to $G = (V, A)$. Let $Z \subset V$ be a set of perturbed nodes and let $\bar{Z} = V \setminus Z$ be the unperturbed nodes. Assume that the joint distribution of Y and the perturbed variables U_Z factorizes as in (30). Then the collection of observed variables $(Y_{\bar{Z}}, U_Z)$ factorizes with respect to the perturbed graph G_Z from Definition 9.*

Proof. We will prove the lemma for discrete random variables. The proof for continuous random variables is identical except that marginalization would be represented by integrals instead of sums.

Let $Z = \{v_1, \dots, v_n\}$, $Z_0 = \emptyset$ and $Z_k = \{v_1, \dots, v_k\}$. We will prove inductively that $(Y_{\bar{Z}_k}, U_{Z_k})$ factorizes with respect to G_{Z_k} .

The base case with $Z_0 = \emptyset$ is immediate since $(Y_{\bar{Z}_0}, U_{Z_0}) = Y$ and $G_{Z_0} = G$. Now assume inductively that $(Y_{\bar{Z}_{k-1}}, U_{Z_{k-1}})$ factorizes with respect to $G_{Z_{k-1}}$ for some $k \geq 1$.

$$P(Y_{\bar{Z}_k}, U_{Z_k}) \quad (31)$$

$$= \sum_{Y_{Z_k}} \prod_{q \in Q} \Psi_q(Y_q) \prod_{i=1}^k \Psi_{v_i, (v_i)_p}(y_{v_i}, u_{v_i}) \quad (32)$$

$$= \sum_{y_{v_k}} \left(\sum_{Y_{Z_{k-1}}} \prod_{q \in Q} \Psi_q(Y_q) \prod_{i=1}^{k-1} \Psi_{v_i, (v_i)_p}(y_{v_i}, u_{v_i}) \right) \Psi_{v_k, (v_k)_p}(y_{v_k}, u_{v_k}) \quad (33)$$

$$= \sum_{y_{v_k}} P(Y_{\bar{Z}_{k-1}}, U_{Z_{k-1}}) \Psi_{v_k, (v_k)_p}(y_{v_k}, u_{v_k}) \quad (34)$$

The first line, (32) follows by marginalizing Y_{Z_k} out of the factorized distribution from (30). Then the terms are regrouped and then (32) is employed for $P(Y_{\bar{Z}_{k-1}}, U_{Z_{k-1}})$.

By induction, we have that $P(Y_{\bar{Z}_{k-1}}, U_{Z_{k-1}})$ factorizes according to a collection of cliques, C , in G_{Z_k} . Let $C_{v_k} \subset C$ be the collection of cliques such that $v_k \in c$ for all $c \in C_{v_k}$. For compact notation, let $X = (Y, U_Z)$. Then the formula for $P(Y_{\bar{Z}_k}, U_{Z_k})$ can be expressed as

$$P(Y_{\bar{Z}_k}, U_{Z_k}) = \left(\sum_{y_{v_k}} \prod_{c \in C_{v_k}} \Psi_c(X_c) \Phi_{v_k, (v_k)_p}(y_{v_k}, u_{v_k}) \right) \prod_{c \in C \setminus C_{v_k}} \Phi_c(X_c). \quad (35)$$

The second term on the right is a collection of factors corresponding to cliques in $G_{Z_{k-1}}$. Now, since $A_{Z_{k-1}} \subset A_{Z_k}$, they must also be cliques of G_{Z_k} . The lemma will be proved if the variables first term on the right correspond to a clique in G_{Z_k} .

Say $i \neq v_k$ and $j \neq v_k$ are nodes corresponding to variables in the sum in (35). Then there must be paths from i to v_k and v_k to j such that any intermediate node is in Z_{k-1} . Now, since $v_k \in Z_k$, there is a path from i to j such that all of the intermediate nodes are in Z_k . Thus, the nodes in the sum form a clique in G_{Z_k} . \square

In our model, we have assumed that the variables corresponding to corrupted nodes, y_i for $i \in Z$, are hidden. Then Lemma 1 shows that marginalizing out the variables y_i introduces new probabilistic relationships between the neighbors of y_i . The new links between variables are precisely described by the perturbed graph construction of Theorem 3. Note that any method that attempts to reconstruct the graphical structure of the Markov random field based only on the observed data that contains corrupt data will be likely to detect spurious relationships.¹

¹In some special cases, it may be possible to exploit prior knowledge of network structure to rule out some spurious links [28].

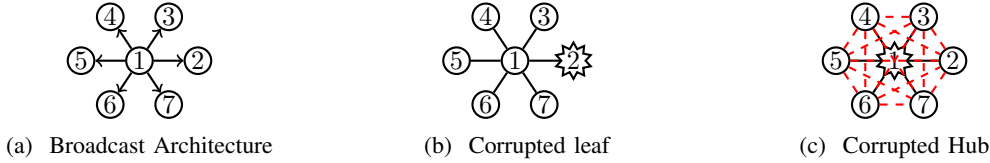


Fig. 4: This figure shows an extreme example of the effect of data corruption of even a single node. 4a shows the original directed graph. 4b shows that even if the leaf is corrupted there are no erroneous links introduced. But if the hub is corrupted as shown in 4c then all the nodes become spuriously correlated.

Below, we will show that if $P(Y_{\bar{Z}}, U_Z)$ is positive everywhere, then the perturbed graph exactly characterizes the conditional independence of the observed nodes. To present this strengthened version of Lemma 1, some definitions are required.

Definition 14 (Pairwise Markov property). *Suppose $G = (V, A)$ is an undirected graph whose N nodes represent random variables y_1, \dots, y_N . Let $Y = \{y_1, \dots, y_N\}$. Pairwise Markov property associated with G holds, if for any non-adjacent vertices i, j , we have that $\text{sep}(i, j | V \setminus \{i, j\})$ implies that y_i and y_j are conditionally independent given $Y \setminus \{y_i, y_j\}$.*

As in the discussion of LTI systems, it is convenient to identify the observed but unperturbed variables $Y_{\bar{Z}}$ with $U_{\bar{Z}}$ so that the collection of observed variables can be denoted by $U = (U_{\bar{Z}}, U_Z)$.

Theorem 4. *Let Y be a set of random variables that factorize according to graph $G = (V, A)$. Suppose, $Z \subset V$, is a set of perturbed nodes such that the joint distribution (Y, U_Z) factorizes as in (30). Let U denote the set of all observed variables and assume that $P(U)$ is positive everywhere. Define $U_{\bar{i}\bar{j}} := U \setminus \{u_i, u_j\}$. Then, $i - j$ is an edge in the perturbed graph, G_Z , if and only if u_i is not conditionally independent of u_j given $U_{\bar{i}\bar{j}}$.*

Proof. From lemma 1 we know that U factorizes according to G_Z . Thus, positivity of $P(U)$ implies that the pairwise Markov property is equivalent to U factorizing according to G_Z . See [27]. Therefore, $\text{sep}(i, j | V \setminus \{i, j\})$ (in G_Z) if and only if $u_i \perp\!\!\!\perp u_j | U_{\bar{i}\bar{j}}$. Note that $\text{sep}(i, j | V \setminus \{i, j\})$ means precisely that $i - j \notin A_Z$. \square

VI. SIMULATION RESULTS

Power spectrum estimates were computed after 10^4 simulation time steps. The estimated spectra were then averaged over 100 trials. The red boxes indicate the erroneous links introduced as a result of the network perturbation in addition to the the links in the true moral graph as indicated by the black boxes. For both the networks, the sequences e_i are zero mean white Gaussian noise.

A. Star Topology

The transfer function for each link is z^{-1} .

1) *Corrupted Leaf:* The perturbation considered here is the random delay model, (11), on node 2:

$$d_2[t] = \begin{cases} 3, & \text{with probability 0.65} \\ 1, & \text{with probability 0.35.} \end{cases}$$

$$\Phi_{uu}^{-1}(z) = \begin{bmatrix} 15.02 & 0.14 & 1.49 & 1.49 & 1.50 & 1.50 & 1.45 \\ 0.14 & 1.74 & 0.05 & 0.05 & 0.05 & 0.05 & 0.04 \\ 1.49 & 0.05 & 2.36 & 0.05 & 0.06 & 0.06 & 0.06 \\ 1.49 & 0.05 & 0.05 & 2.35 & 0.06 & 0.05 & 0.06 \\ 1.50 & 0.05 & 0.06 & 0.06 & 2.36 & 0.05 & 0.05 \\ 1.50 & 0.05 & 0.06 & 0.05 & 0.05 & 2.36 & 0.05 \\ 1.45 & 0.04 & 0.06 & 0.06 & 0.05 & 0.05 & 2.34 \end{bmatrix}$$

As predicted by Theorem 3, perturbation of Node 2 for this architecture does not introduce any erroneous links. See Figure 4b.

2) *Corrupted Hub:* The perturbation considered here is a random delay on the hub node:

$$d_1[t] = \begin{cases} 2, & \text{with probability 0.75} \\ 4, & \text{with probability 0.25.} \end{cases}$$

Theorem 3 predicts that perturbing the central node could introduce erroneous links between all of the nodes. See Figure 4c.

$$\Phi_{uu}^{-1}(z) = \begin{bmatrix} 5.08 & 0.40 & 0.40 & 0.40 & 0.39 & 0.39 & 0.38 \\ 0.40 & 2.07 & 0.27 & 0.27 & 0.27 & 0.26 & 0.27 \\ 0.40 & 0.27 & 2.08 & 0.27 & 0.27 & 0.28 & 0.27 \\ 0.40 & 0.27 & 0.27 & 2.07 & 0.27 & 0.27 & 0.27 \\ 0.39 & 0.27 & 0.27 & 0.27 & 2.07 & 0.27 & 0.27 \\ 0.39 & 0.26 & 0.28 & 0.27 & 0.27 & 2.08 & 0.27 \\ 0.38 & 0.27 & 0.27 & 0.27 & 0.27 & 0.27 & 2.08 \end{bmatrix}$$

B. Chain Topology

The chain topology in Figure 5 is considered. The transfer functions are: between nodes 1 and 2, $1.2 + 0.9z^{-1}$, between nodes 2 and 3, $1 + 0.2z^{-1}$, between nodes 3 and 4, $1 - 0.9z^{-1} + 0.3z^{-2}$ and then for the last link z^{-1} . Figure 5 In the simulations, nodes 2 and 3 are simultaneously corrupted with the random delay models

$$d_2[t] = \begin{cases} 1, & \text{with probability 0.83} \\ 2, & \text{with probability 0.17.} \end{cases}$$

$$d_3[t] = \begin{cases} 2, & \text{with probability 0.85} \\ 4, & \text{with probability 0.15.} \end{cases}$$

$$\Phi_{uu}^{-1}(z) = \begin{bmatrix} 4.23 & 0.54 & 0.12 & 0.25 & 0.05 \\ 0.54 & 1.20 & 0.16 & 0.13 & 0.02 \\ 0.12 & 0.16 & 1.06 & 0.12 & 0.02 \\ 0.25 & 0.13 & 0.12 & 2.22 & 0.90 \\ 0.05 & 0.02 & 0.02 & 0.90 & 1.42 \end{bmatrix}$$

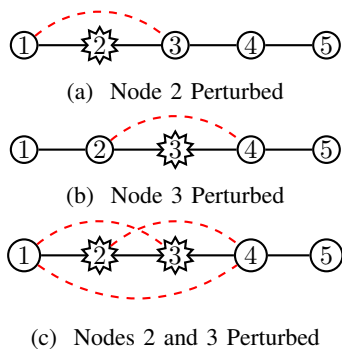


Fig. 5: This figure shows how multiple perturbations can lead to a cascade effect as predicted by Theorem 3. Here the original moral graph is a chain. 5a and 5b show the erroneous edges that can arise from perturbing a single node. If nodes 2 and 3 are both perturbed, then another erroneous link between 1 and 4 must be added.

Perturbation of 2 adds a false relationship between 1 and 3. In addition, perturbation of 3 introduces erroneous relations between the nodes 1 and 4 as well as between 2 and 4. Thus the erroneous relationships could arise between any nodes that are kins of 3 including the already introduced false kins of 3. Despite this cascaded effect the erroneous links remain local in the sense that the dependency of 5 is unaffected.

VII. CONCLUSION

We studied the problem of inferring the network structure of interacting agents from corrupt data-streams. We described general model of data-corruption that introduces an additive term in the power spectra and captures a wide class of measurement uncertainties. We then studied inferring topology of a network of LTI systems from corrupt data-streams. We established that network topology reconstruction from corrupt data streams can result in erroneous links between the nodes. Particularly we provided exact characterization by proving that the erroneous links are localized to the neighborhood of the perturbed node. We then studied the influence of data corruption on Markov random field models. Here we found that our characterization of erroneous links for LTI systems precisely characterized the spurious relationships that can arise in Markov random fields.

Our results show that data corruption gives rise to the appearance of cliques that are localized around the corrupt nodes. Two natural future research directions emerge. The first direction would be to prior structural knowledge to infer the location of corrupt nodes. For example, in some power network problems, cliques cannot be present, and so the appearance of a clique would indicate that data must have been corrupted. The other direction would be to use network reconstruction results of to guide sensor placement algorithms. For example, if the neighborhood of a node forms a clique, then our results suggest that this clique may be due to data corruption, and thus a better sensor could be used to rule out this possibility.

APPENDIX A PROOF OF THEOREM 2

Define the following deviations from the mean: $\Delta A_i[t] = A_i[t] - \bar{A}_i$, $\Delta B_i[t] = B_i[t] - \bar{B}_i$, $\Delta C_i[t] = C_i[t] - \bar{C}_i$, and $\Delta D_i[t] = D_i[t] - \bar{D}_i$

Note that the Lyapunov equation, (9), can be expressed as:

$$P = \bar{A}_i^\top P \bar{A}_i + \mathbb{E}[\Delta A_i[t]^\top P \Delta A_i[t]] + Q \succeq \bar{A}_i^\top P \bar{A}_i + Q. \quad (36)$$

Here $S \preceq T$ denotes that $T - S$ is positive semidefinite. Since a solution must hold for all Q , it must hold, in particular for positive definite Q . Thus, \bar{A}_i must be a stable matrix.

Set $\bar{u}_i[t] = (h_i \star y_i)[t] = \mathbb{E}[u_i[t]|y_i]$, so that $\Delta u_i[t] = u_i[t] - \bar{u}_i[t]$.

With this notation, the cross spectrum, (10b), will be derived:

$$R_{u_i y_i}[t] = \mathbb{E}[u_i[t] y_i[0]] \quad (37)$$

$$= \mathbb{E}[\mathbb{E}[u_i[t] y_i[0] | y_i]] \quad (38)$$

$$= \mathbb{E}[(h_i \star y_i)[t] y_i[0]] \quad (39)$$

$$= (h_i \star R_{y_i y_i})[t]. \quad (40)$$

Here, (38) is due to the tower property of conditional expectation. Then (10b) follows by taking Z -transforms.

Since \bar{A}_i is stable and $y_i[t]$ is wide-sense stationary, we must have that $\bar{u}_i[t]$ is wide-sense stationary.

Note that by construction, $R_{u_i u_i}[t] = R_{\bar{u}_i \bar{u}_i}[t] + R_{\Delta u_i \Delta u_i}[t]$. Furthermore, we must have that

$$R_{\bar{u}_i \bar{u}_i}[t] = (h_i \star R_{y_i y_i} \star h_i^*)[t], \quad (41)$$

where h_i^* is the time-reversed, transposed impulse response. Thus, (10a) holds by taking Z -transforms.

The only part that remains to be proved is that u_i is wide-sense stationary. This will follow as long as $\Delta u_i[t]$ has a finite autocorrelation.

To show that $R_{\Delta u_i \Delta u_i}[t]$ is bounded, we will explicitly construct an expression for it. To derive this expression, we need expressions for the autocorrelation of x_i and the cross correlation between x_i and y_i .

Let $\bar{x}_i[t] = \left(\left[\begin{array}{c|c} \bar{A}_i & \bar{B}_i \\ \hline I & 0 \end{array} \right] \star y_i \right)[t]$ and let $\Delta x_i[t] = x_i[t] - \bar{x}_i[t]$. Note that $\bar{x}_i[t] = \mathbb{E}[x_i[t]|y_i]$. As with \bar{u}_i , we have that $\bar{x}_i[t]$ is wide-sense stationary. Using a derivation identical to that of $R_{u_i y_i}[t]$, we have that the cross correlation of x_i and y_i is given by:

$$R_{x_i y_i}[t] = \left(\left[\begin{array}{c|c} \bar{A}_i & \bar{B}_i \\ \hline I & 0 \end{array} \right] \star R_{y_i y_i} \right)[t] \quad (42)$$

Thus, we see that $R_{x_i x_i}[t] = R_{\bar{x}_i \bar{x}_i}[t]$.

Now we will work out the autocorrelation of x_i . The autocorrelation of $\bar{x}_i[t]$ is given by:

$$R_{\bar{x}_i \bar{x}_i}[t] = \left(\left[\begin{array}{c|c} \bar{A}_i & \bar{B}_i \\ \hline I & 0 \end{array} \right] \star R_{y_i y_i} \star \left[\begin{array}{c|c} \bar{A}_i & \bar{B}_i \\ \hline I & 0 \end{array} \right]^* \right)[t]. \quad (43)$$

By construction, we have that $R_{x_i x_i}[t] = R_{\bar{x}_i \bar{x}_i}[t] + R_{\Delta x_i \Delta x_i}[t]$. The following lemma characterizes the autocorrelations of $\Delta x_i[k]$.

Lemma 2. Assume that a solution to the generalized Lyapunov equation, (9), holds for all Q . Then $R_{\Delta x_i \Delta x_i}[0]$ is uniquely defined by:

$$R_{\Delta x_i \Delta x_i}[0] = \mathbb{E}[A_i[0]R_{\Delta x_i \Delta x_i}[0]A_i[0]^\top] + W + \mathbb{E} \left[\begin{bmatrix} \Delta A_i[0] & \Delta B_i[0] \end{bmatrix} \begin{bmatrix} R_{\bar{x}_i \bar{x}_i}[0] & R_{\bar{x}_i y_i}[0] \\ R_{y_i \bar{x}_i}[0] & R_{y_i y_i}[0] \end{bmatrix} \begin{bmatrix} \Delta A_i[0]^\top \\ \Delta B_i[0]^\top \end{bmatrix} \right]. \quad (44)$$

For $k > 0$,

$$R_{\Delta x_i \Delta x_i}[k] = \bar{A}_i^k R_{\Delta x_i \Delta x_i}[0] \\ R_{\Delta x_i \Delta x_i}[-k] = R_{\Delta x_i \Delta x_i}[k]^\top.$$

Proof. For $k > 0$ we have

$$\begin{aligned} R_{\bar{x}_i \bar{x}_i}[k] + R_{\Delta x_i \Delta x_i}[k] &= \mathbb{E}[x_i[k]x_i[0]^\top] \\ &= \mathbb{E}[(A_i[k-1]x_i[k-1] + B_i[k-1]y_i[k-1])x_i[0]^\top] \\ &= \bar{A}_i R_{x_i x_i}(k-1) + \bar{B}_i R_{y_i x_i}(k-1) \\ &= (\bar{A}_i R_{\bar{x}_i \bar{x}_i}(k-1) + \bar{B}_i R_{y_i x_i}(k-1)) \\ &\quad + \bar{A}_i R_{\Delta x_i \Delta x_i}(k-1) \\ &= R_{\bar{x}_i \bar{x}_i}[k] + \bar{A}_i R_{\Delta x_i \Delta x_i}[k-1]. \end{aligned}$$

Thus, the formula for $R_{\Delta x_i \Delta x_i}[k]$ holds for $k \neq 0$. (The expression for $k < 0$ follows from transposing.)

Note that

$$\begin{aligned} \Delta x_i[k+1] &= (\bar{A}_i + \Delta A_i[k])(\bar{x}_i[k] + \Delta x_i[k]) + (\bar{B}_i + \Delta B_i[k])y_i[k] \\ &\quad + w_i[k] - \bar{A}_i \bar{x}_i[k] - \bar{B}_i y_i[k] \\ &= A_i[k]\Delta x_i[k] + \Delta A_i[k]\bar{x}_i[k] + \Delta B_i[k]y_i[k] + w_i[k]. \end{aligned}$$

Furthermore, note that $\Delta x_i[k]$ is independent of $\Delta A_i[k]$ and $\Delta B_i[k]$. The expression for $R_{\Delta x_i \Delta x_i}(0)$ follows by setting $\mathbb{E}[\Delta x_i[k+1]\Delta x_i[k+1]^\top] = \mathbb{E}[\Delta x_i[k]\Delta x_i[k]^\top]$.

Note that $R_{\Delta x_i \Delta x_i}(0)$ can be computed from (9) with

$$Q = W + \mathbb{E} \left[\begin{bmatrix} \Delta A_i[0] & \Delta B_i[0] \end{bmatrix} \begin{bmatrix} R_{\bar{x}_i \bar{x}_i}(0) & R_{\bar{x}_i y_i}(0) \\ R_{y_i \bar{x}_i}(0) & R_{y_i y_i}(0) \end{bmatrix} \begin{bmatrix} \Delta A_i[0]^\top \\ \Delta B_i[0]^\top \end{bmatrix} \right] \quad (45)$$

□

As discussed above, the proof of the theorem will be completed once the autocorrelation of Δu_i is characterized. The following lemma gives the desired characterization.

Lemma 3. For $k = 0$, $R_{\Delta u_i \Delta u_i}[0]$ is given by

$$R_{\Delta u_i \Delta u_i}[0] = \bar{C}_i R_{\Delta x_i \Delta x_i}[0] \bar{C}_i^\top + V + \mathbb{E} \left[\begin{bmatrix} \Delta C_i[0] & \Delta D_i[0] \end{bmatrix} \begin{bmatrix} R_{x_i x_i}[0] & R_{x_i y_i}[0] \\ R_{y_i x_i}[0] & R_{y_i y_i}[0] \end{bmatrix} \begin{bmatrix} \Delta C_i[0]^\top \\ \Delta D_i[0]^\top \end{bmatrix} \right] \quad (46)$$

For $k > 0$, $R_{\Delta u_i \Delta u_i}[k]$ is given by

$$\begin{aligned} R_{\Delta u_i \Delta u_i}[k] &= \bar{C}_i R_{\Delta x_i \Delta x_i}[k] \bar{C}_i^\top + \bar{C}_i \bar{A}_i^{k-1} S \\ &\quad + \bar{C}_i \bar{A}_i^{k-1} \mathbb{E} \left[\begin{bmatrix} \Delta A_i[0] & \Delta B_i[0] \end{bmatrix} \begin{bmatrix} R_{x_i x_i}[0] & R_{x_i y_i}[0] \\ R_{y_i x_i}[0] & R_{y_i y_i}[0] \end{bmatrix} \begin{bmatrix} \Delta C_i[0]^\top \\ \Delta D_i[0]^\top \end{bmatrix} \right]. \end{aligned} \quad (47)$$

For $k < 0$, $R_{\Delta u_i \Delta u_i}[k] = R_{\Delta u_i \Delta u_i}[-k]$.

Proof. Note that $\Delta u_i[k]$ can be decomposed as:

$$\Delta u_i[k] \quad (48)$$

$$= u_i[k] - \bar{u}_i[k] \quad (49)$$

$$= (\bar{C}_i + \Delta C_i[k])(\bar{x}_i[k] + \Delta x_i[k]) + (\bar{D}_i + \Delta D_i[k])y_i[k] + v_i[k] - \bar{C}_i \bar{x}_i[k] - \bar{D}_i y_i[k] \quad (50)$$

$$= \bar{C}_i \Delta x_i[k] + \Delta C_i[k]x_i[k] + \Delta D_i[k]y_i[k] + v_i[k] \quad (51)$$

$$= \bar{C}_i \Delta x_i[k] + \Delta C_i[k]x_i[k] + \Delta D_i[k]y_i[k] + v_i[k] \quad (52)$$

As before, $\Delta x_i[k]$ is independent of $\Delta C_i[k]$ and $\Delta D_i[k]$. Thus, the expression for $R_{\Delta u_i \Delta u_i}[0]$ follows by computing $\mathbb{E}[\Delta u_i[k]^2]$.

For $k > 0$, note that $\Delta C_i[k]$ and $\Delta D_i[k]$ are independent of $\Delta C_i[0]$ and $\Delta D_i[0]$. However, $\Delta x_i[k]$ may be correlated with $\Delta C_i[0]$, $\Delta D_i[0]$, and $v_i[0]$. So, multiplying the expression from (52) for $k > 0$ and $k = 0$ and dropping the $\Delta C_i[k]$ and $\Delta D_i[k]$ terms gives

$$\begin{aligned} R_{\Delta u_i \Delta u_i}(k) &= \mathbb{E} [\bar{C}_i \Delta x_i[k] (\bar{C}_i \Delta x_i[0] +)^\top] \\ &\quad + \mathbb{E} [\bar{C}_i \Delta x_i[k] (\Delta C_i[0]x_i[0] + \Delta D_i[0]y_i[0] + v_i[0])^\top] \end{aligned} \quad (53)$$

$$= \bar{C}_i R_{\Delta x_i \Delta x_i}(k) \bar{C}_i^\top \quad (54)$$

$$+ \bar{C}_i \mathbb{E} [\Delta x_i[k] (\Delta C_i[0]x_i[0] + \Delta D_i[0]y_i[0] + v_i[0])^\top] \quad (55)$$

Let $A_i[j : k]$ be the product defined by $A_i[k : k] = I$ and $A_i[j : k] = A_{i,j}[k-1]A_{i,j}[k-2] \cdots A_{i,j}[j]$ for $j < k$. An induction argument shows that

$$\begin{aligned} x_i[k] &= A_i[0 : k]x_i[0] + \sum_{j=0}^{k-1} A_i[j+1 : k](B_i[j]y_i[j] + w_i[j]) \\ &= A_i[1 : k]A_i[0]x_i[0] + B_i[0]y_i[0] + w_i[0] + \\ &\quad + \sum_{j=1}^{k-1} A_i[j+1 : k](B_i[j]y_i[j] + w_i[j]). \end{aligned}$$

Let \mathcal{F} be the σ -algebra generated by y_i and all of the random terms $(A_i[j], B_i[j], C_i[j], D_i[j], w_i[j], v_i[j])$ for $i \leq 0$. Then the expression for $x_i[k]$ implies that

$$\begin{aligned} \mathbb{E}[x_i[k]|\mathcal{F}] &= \sum_{j=1}^{k-1} \bar{A}^{k-1-j} \bar{B} y_i[j] \\ &\quad + \bar{A}^{k-1} ((\bar{A} + \Delta A_i[0])x_i[0] + (\bar{B} + \Delta B_0)y_i[0] + w_i[0]) \\ &= \bar{x}_i[k] + \bar{A}^{k-1} \bar{A} \Delta x_i[0] + \\ &\quad + \bar{A}^{k-1} (\Delta A_i[0]x_i[0] + \Delta B_i[0]y_i[0] + w_i[0]). \end{aligned}$$

Using the tower property gives:

$$\begin{aligned} & \mathbb{E}[\Delta x_i[k](\Delta C_i[0]x_i[0] + \Delta D_i[0]y_i[0] + v_i[0])^\top] \\ &= \mathbb{E}[\mathbb{E}[\Delta x_i[k](\Delta C_i[0]x_i[0] + \Delta D_i[0]y_i[0] + v_i[0])^\top | \mathcal{F}]] \\ &= \bar{A}^{k-1} \mathbb{E}[(\Delta A_i[0]x_i[0] + \Delta B_i[0]y_i[0] + w_i[0]) \\ &\quad \cdot (\Delta C_i[0]x_i[0] + \Delta D_i[0]y_i[0] + v_i[0])^\top], \end{aligned}$$

where the last equality used that $\Delta x_i[0]$ is independent of $\Delta A_i[0]$, $\Delta B_i[0]$, and $v_i[0]$. Combining this result with (54) gives the desired expression for $R_{\Delta u \Delta u}(k)$. The expression for $R_{\Delta u \Delta u}(-k)$ follows because $\Delta u_i[k]$ is a real scalar. \square

REFERENCES

- [1] J. Fan, J. Meng, Y. Ashkenazy, S. Havlin, and H. J. Schellnhuber, "Network analysis reveals strongly localized impacts of el niño," *Proceedings of the National Academy of Sciences*, 2017.
- [2] J. S. Kaufman, *Methods in social epidemiology*. John Wiley & Sons, 2017, vol. 16.
- [3] D. S. Bassett and O. Sporns, "Network neuroscience," *Nature neuroscience*, vol. 20, no. 3, p. 353, 2017.
- [4] A. A. Julius and C. Belta, "Genetic regulatory network identification using monotone functions decomposition," *IFAC Proceedings Volumes*, vol. 44, no. 1, pp. 11785–11790, 2011.
- [5] P. Giudici and A. Spelta, "Graphical network models for international financial flows," *Journal of Business & Economic Statistics*, vol. 34, no. 1, pp. 128–138, 2016.
- [6] D. Y. Kenett and S. Havlin, "Network science: a useful tool in economics and finance," *Mind & Society*, vol. 14, no. 2, pp. 155–167, 2015.
- [7] C. Perera, A. Zaslavsky, P. Christen, and D. Georgakopoulos, "Context aware computing for the internet of things: A survey," *IEEE communications surveys & tutorials*, vol. 16, no. 1, pp. 414–454, 2014.
- [8] D. Guinard, V. Trifa, S. Karnouskos, P. Spiess, and D. Savio, "Interacting with the soa-based internet of things: Discovery, query, selection, and on-demand provisioning of web services," *IEEE Transactions on Services Computing*, vol. 3, no. 3, pp. 223–235, 2010.
- [9] Y. Wang, T. Tan, and K.-F. Loe, "Video segmentation based on graphical models," in *Computer Vision and Pattern Recognition, 2003. Proceedings. 2003 IEEE Computer Society Conference on*, vol. 2. IEEE, 2003, pp. II-335.
- [10] D. Deka, S. Backhaus, and M. Chertkov, "Structure learning in power distribution networks," *IEEE Transactions on Control of Network Systems*, vol. 5, no. 3, pp. 1061–1074, Sept 2018.
- [11] M. S. Stankovic, S. S. Stankovic, and K. H. Johansson, "Distributed time synchronization for networks with random delays and measurement noise," *Automatica*, vol. 93, pp. 126 – 137, 2018.
- [12] H.-H. Cho, C.-Y. Chen, T. K. Shih, and H.-C. Chao, "Survey on underwater delay/disruption tolerant wireless sensor network routing," *IET Wireless Sensor Systems*, vol. 4, no. 3, pp. 112–121, 2014.
- [13] A. S. Leong, S. Dey, and D. E. Quevedo, "Sensor scheduling in variance based event triggered estimation with packet drops," *IEEE Transactions on Automatic Control*, vol. 62, no. 4, pp. 1880–1895, 2017.
- [14] H. H. Weerts, P. M. V. den Hof, and A. G. Dankers, "Identifiability of linear dynamic networks," *Automatica*, vol. 89, pp. 247 – 258, 2018.
- [15] J. M. Hendrickx, M. Gevers, and A. S. Bazanella, "Identifiability of dynamical networks with partial node measurements," *IEEE Transactions on Automatic Control*, 2018.
- [16] H. J. Van Waarde, P. Tesi, and M. K. Camlibel, "Necessary and sufficient topological conditions for identifiability of dynamical networks," *IEEE Transactions on Automatic Control*, 2019.
- [17] J. Etesami, N. Kiyavash, and T. Coleman, "Learning minimal latent directed information polytrees," *Neural computation*, vol. 28, no. 9, pp. 1723–1768, 2016.
- [18] F. Sepehr and D. Materassi, "Blind learning of tree network topologies in the presence of hidden nodes," *IEEE Transactions on Automatic Control*, 2019.
- [19] D. Materassi and M. V. Salapaka, "On the problem of reconstructing an unknown topology via locality properties of the wiener filter," *IEEE transactions on automatic control*, vol. 57, no. 7, pp. 1765–1777, 2012.
- [20] C. J. Quinn, N. Kiyavash, and T. P. Coleman, "Directed Information Graphs," *IEEE Transactions on Information Theory*, vol. 61, no. 12, pp. 6887–6909, 2015.

- [21] Y. Yuan, G. B. Stan, S. Warnick, and J. Goncalves, "Robust dynamical network structure reconstruction," *Automatica*, vol. 47, no. 6, pp. 1230 – 1235, 2011, special Issue on Systems Biology.
- [22] V. Chetty, D. Hayden, J. Goncalves, and S. Warnick, "Robust signal-structure reconstruction," in *52nd IEEE Conference on Decision and Control*, Dec 2013, pp. 3184–3189.
- [23] J. Goncalves and S. Warnick, "Necessary and sufficient conditions for dynamical structure reconstruction of lti networks," *IEEE Transactions on Automatic Control*, vol. 53, no. 7, pp. 1670–1674, Aug 2008.
- [24] V. R. Subramanian, A. Lamperski, and M. V. Salapaka, "Network topology identification from corrupt data streams," in *IEEE 56th Annual Conference on Decision and Control (CDC)*, 2017, pp. 1695–1700.
- [25] D. Koller and N. Friedman, *Probabilistic Graphical Models: Principles and Techniques*. The MIT Press, 2009.
- [26] K. B. Petersen and M. S. Pedersen, "The matrix cookbook," 2012. [Online]. Available: <http://www2.imm.dtu.dk/pubdb/p.php?3274>.
- [27] S. L. Lauritzen, *Graphical models*. Oxford :: Clarendon Press, 1996.
- [28] S. Talukdar, D. Deka, D. Materassi, and M. Salapaka, "Exact topology reconstruction of radial dynamical systems with applications to distribution system of the power grid," in *2017 American Control Conference (ACC)*, 2017, pp. 813–818.



Venkat Ram Subramanian received the B.Tech degree in electrical engineering from SRM University, Chennai, India, in 2014, and the M.S. degree in electrical engineering from the University of Minnesota, Minneapolis, in 2016.

Currently, he is working towards a Ph.D. degree at the University of Minnesota. His Ph.D. research is on learning dynamic relations in networks from corrupt data-streams. In addition to system identification and stochastic systems, his research interests also include optimal control and graphical models.



Andrew Lamperski (S'05–M'11) received the B.S. degree in biomedical engineering and mathematics in 2004 from the Johns Hopkins University, Baltimore, MD, and the Ph.D. degree in control and dynamical systems in 2011 from the California Institute of Technology, Pasadena. He held postdoctoral positions in control and dynamical systems at the California Institute of Technology from 2011–2012 and in mechanical engineering at The Johns Hopkins University in 2012. From 2012–2014, did postdoctoral work in the Department of Engineering,

University of Cambridge, on a scholarship from the Whitaker International Program. In 2014, he joined the Department of Electrical and Computer Engineering, University of Minnesota as an Assistant Professor. His research interests include optimal control, optimization, and identification, with applications to neuroscience and robotics.



Murti Salapaka (SM'01–F'19) Murti Salapaka received the bachelors degree from the Indian Institute of Technology, Madras, India, in 1991, and the Masters and Ph.D. degrees from the University of California, Santa Barbara, CA, USA, in 1993 and 1997, respectively, all in mechanical engineering. He was with Electrical Engineering department, Iowa State University, from 1997 to 2007. He is currently the Vincentine Hermes-Luh Chair Professor with the Electrical and Computer Engineering Department, University of Minnesota, Minneapolis, MN, USA.

Prof. Salapaka was the recipient of the NSF CAREER Award and the ISU Young Engineering Faculty Research Award for the years 1998 and 2001, respectively. He is an IEEE Fellow.